Proceedings of the Twenty-eighth (2018) International Ocean and Polar Engineering Conference
Sapporo, Japan, June 10-15, 2018

ISBN 978-1-880653-87-6; ISSN 1098-6189

www.isope.org

Hull Form Optimization Design of KCS at Full Speed Range Based on Resistance Performance in Calm Water

*Xinwang Liu, Jinkai Wang, Decheng Wan**
State Key Laboratory of Ocean Engineering, School of Naval Architecture, Ocean and Civil Engineering, Shanghai Jiao Tong University,
Collaborative Innovation Center for Advanced Ship and Deep-Sea Exploration, Shanghai, China
*Corresponding author

ABSTRACT

In this paper, the KCS is considered as the parent ship. The single-objective genetic algorithm is taken as the optimization technique leading to an optimal ship considering full speed range. In order to validate and analyze the optimization results, numerical calculation of the optimal ship at full speed range is further carried out and also compared with that of the parent ship. The results show that the resistance performance of the optimal ship at full speed range is much better. It turns out that OPTShip-SJTU has practical applications in the aspect of probability optimization of ship hydrodynamic performances.

KEY WORDS: Wave-making resistance; hull form optimization; full-speed-range optimization; NMShip-SJTU; OPTShip-SJTU.

INTRODUCTION

In the process of ship design, hull form design is of vital importance. The design level of ship hull form has a great influence on its hydrodynamic performances and economic efficiency of the ship. In recent years, with the vigorous development of computer technology and the continuous improvement of the calculation theory, the Simulation-Based-Design (SBD) technology is becoming possible. It is a new design method which integrates hull form transformation method, optimization technology and numerical calculation module. The technique uses geometric reconstruction method to transform and express hull form, and then predicts the hydrodynamic performance of each hull form scheme with computational fluid dynamic methods. Finally, the optimal hull satisfying the constraint condition is obtained by the optimization algorithm.

Current studies are usually aiming at obtaining an optimal hull form at a specific design speed or considering its uncertainty of speed perturbation using single-objective optimization algorithms, or at several different speeds using multi-objective optimization algorithms. However, the ship is unlikely to sail at a certain speed in different needs or environmental conditions. What's more, the speed of the ship can have great influence on the ship resistance as well as other performances, and the weight factors of multi-objective optimization problems are not easy to determine scientifically. Therefore, it is necessary to conduct the optimal design of ship hull at full speed range based on resistance performance in calm water.

In general, there are two kinds of methods for ship's resistance performance prediction. One is the methods based on the potential flow theory and the other is the methods based on computational fluid dynamics(CFD) considering viscosity. Although CFD has developed rapidly in recent years, the methods based on potential flow theory still have their future. The main reason is that in the ship preliminary design stage, designers need to quickly and accurately evaluate the resistance performance of the hull forms in order to do hull form design or optimization. One of the potential flow methods is Neumann-Michell theory (NM theory) (Noblesse et al.,2013), based on the Neumann-Kelvin theory (NK theory). NM theory eliminate the ship waterline integral item in the NK theory, and the whole calculation can be converted to the integral on the wet surface of the ship. The theory adopts the coordination linear flow model and there's no need to solve the distribution on the boundary of the source but calculate the wave resistance through the iteration of velocity potential. Besides, there are a lots of research about comparisons of experimental measurements of wave drag with numerical predictions obtained using the NM theory for the Wigley hull, the Series 60 and DTMB 5415 model. Zhang et al. (2015) used self-developed the NMShip -SJTU solver based on NM theory and calculated the resistance of catamaran, including the resistance of Delft catamaran and Series 60 catamaran in different demihull spacings. The results showed that the calculation results are in good agreement with experimental measurements. Wu et al. (2017) succeed to optimize hull form of a naval surface combatant with the best wave resistance performance evaluated by NM theory. Liu et al. (2017) simulates the wave interference caused by the horizontal and the longitudinal demihull spacings of the quadramarans using NM theory. Yang et al. (2013) presented that the sum of the ITTC friction resistance and the NM theory wave resistance could be expected to yield realistic practical estimates, which could be useful for routine applications to design and ship hull form optimization of a broad range of displacement ships. The computation of the steady flow around a moving ship based on NM theory is efficient and robust due to the succinctness of this theory, and

Kim et al. (2009) pointed that the wave resistance predicted by NM theory is in fairly good agreement with experimental measurements. Using NM theory can quickly complete the resistance performance forecast on personal computers. Calculating the resistance of the ship based on CFD, by contrast, takes more time. For further investigation of the initial set of solutions, the CFD method can be used to obtain more precise flow field information.

In order to save computational costs, one alternative method is to construct a relatively simple surrogate model instead of the complicated numerical analysis of a large number of sample points in order to find the relationship, which is often with strong nonlinearity, between the design variables (input) and the objective functions (output). The surrogate model expresses the relationship between the design variables and the objective functions using a stochastic Gaussian process. The model requires very little time to evaluate the objective function. The most widely used surrogate model are the polynomial-based model, the response surface model, the Kriging model.

In this paper, the KRISO Container Ship (KCS) is considered as the initial ship. The hull form can be globally deformed while the wetted surface area and displacement are constrained within a certain range. The probability distribution function of the speed is given and the mathematical expectation of total resistance in calm water at full speed range is regarded as the objective function. An in-house potential theory-based solver NMShip-SJTU and a practical hydrodynamic optimization tool OPTShip-SJTU are applied for the hull form optimization. Here, the free-form deformation (FFD) method is used as parametric hull surface modification techniques in order to generate a series of hull forms subjected to geometric constraints. The parameters of the sample deformed hull forms are generated by the OLHS approach and their resistances in calm water are calculated by NMShip-SJTU solver.

Hull form optimization is comprehensive technology. The OPTShip-SJTU solver is a self-developed tool based on C++ language for the ship hull form optimization, which has obtained national software copyright. It integrates with a hull surface modification module, a hydrodynamic performance evaluation module, a surrogate module and an optimization module, which can achieve the ship hull form optimization design automatically. The framework of OPTShip-SJTU is shown in Fig. 1.

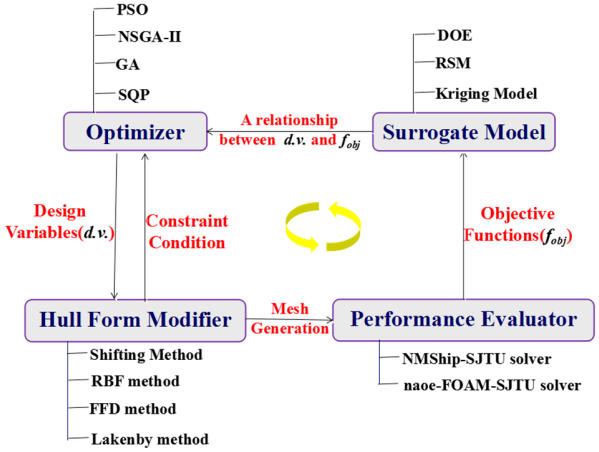

Fig. 1 Framework diagram of OPTShip-SJTU

OPTIMIZATION THEORIES

Hull Form Modification

Ship hull form transformation module is a bridge connecting ship performance evaluation module and optimization module. When the optimization module selects a new series of variables for the design, ship transformation module needs to make rapid response to the certain set of optimization design variables and send them to the ship hydrodynamic performance evaluation module, evaluation results will further affect the optimization module of design. The free surface deformation method FFD is a free mesh deformation method proposed by Sederberg and Parry (1986). It has been widely used in various fields including hull geometry reconstruction and other transportation tools. The basic idea is as follows.

Firstly, a local coordinate system is constructed in a cube containing the object to be deformed. *O '-STU* constructs a local coordinate system, as shown in Fig. 2.

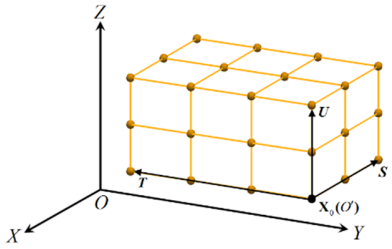

Fig. 2 Local coordinate system of FFD method

Where *O* is the origin of the local coordinate system, *S*, *T*, and *U* are axes vectors along three axes in the local coordinate system. It is obvious, such as the coordinates of *X* in Descartes *O-XYZ*, in a local coordinate system for (*s, t, U*), we have:

$$\mathbf{X} = \mathbf{X}_0 + s\mathbf{S} + t\mathbf{T} + u\mathbf{U} \tag{1}$$

where X_0 is the origin of the local coordinate system, and *s*, *t*, and *u* can be obtained as:

$$s = \frac{\mathbf{T}\times\mathbf{U}\cdot(\mathbf{X}-\mathbf{X}_0)}{\mathbf{T}\times\mathbf{U}\cdot\mathbf{S}},\quad t = \frac{\mathbf{S}\times\mathbf{U}\cdot(\mathbf{X}-\mathbf{X}_0)}{\mathbf{S}\times\mathbf{U}\cdot\mathbf{T}},\quad u = \frac{\mathbf{S}\times\mathbf{T}\cdot(\mathbf{X}-\mathbf{X}_0)}{\mathbf{S}\times\mathbf{T}\cdot\mathbf{U}} \tag{2}$$

Obviously, the values of *s*, *t*, and *u* are between 0 and 1.

In cuboid structure, the control points $\mathbf{Q}_{i,j,k}$, can be easily got by the following expression and can be seen as yellow dots in Fig.2.

$$\mathbf{Q}_{i,j,k} = \mathbf{O}' + \frac{i}{l}\mathbf{S} + \frac{j}{m}\mathbf{T} + \frac{k}{n}\mathbf{U} \tag{3}$$

where $i = 0,1,\cdots,l; j = 0,1,\cdots,m; j = 0,1,\cdots,n$.

Therefore, any point **X** in the framework of Descartes coordinates can be controlled by the control points for:

$$\mathbf{X}(s,t,u) = \sum_{i=0}^{l}\sum_{j=0}^{m}\sum_{k=0}^{n} B_{i,l}(s)B_{j,m}(t)B_{k,n}(u)\mathbf{Q}_{i,j,k} \tag{4}$$

where *B* represents for the Bernstein polynomial basis function:

$$B_{i,n}(u) = \frac{n!}{i!(n-i)!}u^i(1-u)^{n-i} \tag{5}$$

It can be seen from Eq. 4~5 that the initial hull mesh is the linear function of all the control points. After setting up the relation between the geometry and the frame of the ship, we will take the position of some control nodes as the design optimization variables, and then achieve the goal of ship type transformation through the deformation of the control frame. Suppose that the local coordinates of the *X* in the original control framework are (*s*, *t*, *u*), and that the control points $\mathbf{Q}_{i,j,k}$ are changed to

obtain new control nodes $\mathbf{Q}'_{i',j',k'}$, and then the point X will move to point $\mathbf{X}_{ffd}$:

$$\mathbf{X}_{ffd} = \sum_{i=0}^{l}\sum_{j=0}^{m}\sum_{k=0}^{n} B_{i,l}(s)B_{j,m}(t)B_{k,n}(u)\mathbf{Q}'_{i,j,k} \tag{6}$$

By changing the number, direction and size of the control points, different new meshes of the hull can be obtained.

Hydrodynamic Performance Evaluation

Assume a model based on potential flow: a ship of length L_s that steadily advances at speed V_s along a straight path in calm water without viscosity of effectively infinite depth and lateral extent. We define the Froude number $Fr \equiv V_s/\sqrt{gL_s}$ where g is the acceleration of gravity.

The flow about the ship hull is observed from a righthanded moving system of orthogonal coordinates $\mathbf{X}\equiv(X,Y,Z)$ attached to the ship(the X axis is chosen along the path of the ship and points toward the ship bow; the Y axis is parallel to the mean(undisturbed) free surface and points toward the right side of te ship; and the Z axis is vertical and points upward, with the mean free surface taken as the plane $Z = 0$, as shown in Fig.1),and thus appears steady with flow velocity given by the sum of an apparent uniform current $(-V_s, 0, 0)$ opposing the ship speed V_s and the (disturbance) flow velocity $\mathbf{U} \equiv (U, V, W)$ due to the ship. The ship length L_s and speed V_s are used to define nondimensional coordinates $\mathbf{x}\equiv\mathbf{X}/L_s$, flow velocity $\mathbf{u}\equiv\mathbf{U}/V_s$, and flow potential $\phi\equiv\Phi/(V_sL_s)$.

We define points $\mathbf{x}\equiv(x,y,z)$ (which are 'boundary points' located on the ship hull surface Σ^H)and $\tilde{\mathbf{x}}\equiv(\tilde{x},\tilde{y},\tilde{z})$ (which are 'flow-field points' that may be located on the ship hull surface Σ^H or in the flow region outside Σ^H)associated with a Green function $G(\tilde{\mathbf{x}};\mathbf{x})$ that satisfies the Poisson equation that is used to formulate a boundary-integral flow representation:

$$\nabla^2 G(\tilde{\mathbf{x}};\mathbf{x}) = \delta(x-\tilde{x})\delta(\mathrm{y}-\tilde{y})\delta(\mathrm{z}-\tilde{z}) \tag{7}$$

where $\delta(x-\tilde{x})$ represents the Dirac function, which is a singular function and can be defined by integral form:

$$\int_a^b \delta(x-\tilde{x})f(x)dx = \begin{Bmatrix} f(\tilde{x}) \\ 0 \end{Bmatrix} \; if \; \begin{Bmatrix} a<\tilde{x}<b \\ \tilde{x}<a \; or \; b<\tilde{x} \end{Bmatrix} \tag{8}$$

Here, $f(\tilde{x})$ represents the function that is continuous at $x = \tilde{x}$. Eq. 8 can also be extended to higher dimensions:

$$\int_D \delta(x-\tilde{x})\delta(y-\tilde{y})\delta(z-\tilde{z})f(\mathbf{x})dv = \begin{Bmatrix} f(\tilde{\mathbf{x}}) \\ 0 \\ f(\tilde{\mathbf{x}})/2 \end{Bmatrix} \; if \; \begin{Bmatrix} \tilde{\mathbf{x}}\in D \\ \tilde{\mathbf{x}}\notin D \\ \tilde{\mathbf{x}}\in \Sigma \end{Bmatrix} \tag{9}$$

where $f(\mathbf{x})\equiv f(x,y,z), f(\tilde{\mathbf{x}})\equiv f(\tilde{x},\tilde{y},\tilde{z})$, $dv = \mathrm{d}x\mathrm{d}y\mathrm{d}z$, and Σ is the envelope plane of the region D.

The flow potential at a flow-field point $\tilde{\mathbf{x}}$ or at a boundary point $\mathbf{X}$ is identified as $\tilde{\phi}\equiv\phi(\tilde{\mathbf{x}})$ or $\phi\equiv\phi(\mathbf{x})$ respectively. The flow velocities can be obtained by $\tilde{\mathbf{u}}\equiv(\tilde{u},\tilde{v},\tilde{w})\equiv\nabla\tilde{\phi}$ and $\mathbf{u}\equiv(u,v,w)\equiv\nabla\phi$. Furthermore, da denotes the differential element of area at a point $\mathbf{X}$ of the ship hull surface Σ^H, and $\mathbf{n}\equiv(n^x,n^y,n^z)$ is a unit vector that is normal to Σ^H at $\mathbf{X}$ and points outside Σ^H,as shown in Fig. 3.

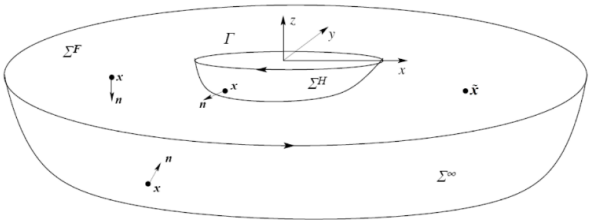

Fig. 3 Coordinate system and boundary sketch

The Neumann-Michell potential representation is expressed as below, and more details of this theory can be found in the reference related.

$$\tilde{\phi} \approx \tilde{\phi}_H + \tilde{\psi}^W \equiv \tilde{\phi}_H^L + \tilde{\phi}_H^W + \tilde{\psi}^W \tag{10}$$

The (modified) Hogner potential $\tilde{\phi}_H$ and the NM correction potential $\tilde{\psi}^W$ can be extended as follows:

$$\tilde{\phi}_H \equiv \int_{\Sigma^H} G\, n^x \, da - \int_{\Sigma^F} G\, \pi^\phi \, dxdy \tag{11}$$

$$\tilde{\psi}^W \equiv \int_{\Sigma^H} (\phi_{t'}\mathbf{d}_* + \phi_{d'}\mathbf{t}_*)\cdot\mathbf{W}da \tag{12}$$

where

Σ^H is the average wet surface area;

G is the Green function;

n^x is the projection in x direction of $\mathbf{n} = (n^x, n^y\, n^z)$;

$\pi^\phi \equiv \phi_z + Fr^2\phi_{xx}$, Fr is the Froude number;

$\mathbf{t}'$ and $\mathbf{d}'$ are two-unit vectors tangent to the ship surface Σ^H. For instance, the unit vectors can be chosen as

$$\mathbf{d}' = (0, -\nu^z, \nu^y), \quad \mathbf{t}' = (\nu, -n^x\nu^y, -n^x\nu^z), \quad \nu \equiv \sqrt{(n^y)^2 + (n^z)^2}, \quad (\nu^y, \nu^z) \equiv (n^y, n^z)/\nu \tag{13}$$

$\phi_{t'}$ and $\phi_{d'}$ are the components of the velocity of the flow field on the wet surface of the ship at the directions of $\mathbf{t}'$ and $\mathbf{d}'$,

$$\begin{cases} \phi_{t'} \equiv \partial\phi/\partial t' \equiv \mathbf{t}'\cdot\nabla\phi \equiv t'^x\phi_x + t'^y\phi_y + t'^z\phi_z \\ \phi_{d'} \equiv \partial\phi/\partial d' \equiv \mathbf{d}'\cdot\nabla\phi \equiv d'^x\phi_x + d'^y\phi_y + d'^z\phi_z \end{cases} \tag{14}$$

Wave function satisfies $G = W + L$, $\nabla\times\mathbf{W} = \nabla W$ and we can get

$$\mathbf{d}_* \equiv \frac{\mathbf{n}\times\mathbf{t}' - \varepsilon\mathbf{n}\times\mathbf{d}'}{1-\varepsilon^2}, \quad \mathbf{t}_* \equiv \frac{\mathbf{n}\times\mathbf{d}' - \varepsilon\mathbf{n}\times\mathbf{t}'}{1-\varepsilon^2}, \quad \varepsilon \equiv \mathbf{t}'\cdot\mathbf{d}' \tag{15}$$

NMShip-SJTU solver is based on the theory of Neumann-Michell theory, and it's developed using C++ language (Zhang and Wan,2015). The input file contains the ship grid, free surface grid and grid type parameter, and we can get surface pressure distribution and resistance of the ship and wave pattern of the free surface, etc.

Surrogate Model Construction

As a kind of regression model, Kriging model is able to exploit the spatial correlation of data in order to predict the shape of the objective function based only on limited information (Sykulski et al.,2011). Kriging exploits the spatial correlation of data in order to build interpolation; therefore, the correlation function is a critical element. This model combines a global model and a local component:

$$y(\mathbf{x}) = f(\mathbf{x}) + z(\mathbf{x}) \tag{16}$$

where $y(\mathbf{x})$ is the unknown real function, $f(\mathbf{x})$ is a known approximation function, and $z(\mathbf{x})$ is the realization of a stochastic process with mean zero, variance σ^2, and non-zero covariance. With $f(\mathbf{x})$ and $z(\mathbf{x})$, the

Kriging model can be built to represent the relationship between the input variables and output variables.
The Kriging predictor is given by:

$$\hat{y} = \hat{\beta} + \mathbf{r}^T(\mathbf{x})\mathbf{R}^{-1}\left(\mathbf{y} - \mathbf{f}\hat{\beta}\right) \tag{17}$$

where $\hat{y}$ is an n_s -dimensional vector that contains the sample values of the response; $\mathbf{f}$ is a column vector of length n_s that is filled with ones when $\mathbf{f}$ is taken as a constant, that is $\mathbf{f}_{n_s\times 1} = [1,1,\cdots,1]^T = \mathbf{1}$; $\mathbf{r}^T(\mathbf{x})$ is the correlation vector of length n_s between an untried $\mathbf{x}$ and the sampled data points $\left\{\mathbf{x}^{(1)},\mathbf{x}^{(2)},\cdots,\mathbf{x}^{(n_s)}\right\}$ and is expressed as:

$$\mathbf{r}^T(\mathbf{x}) = \left[R\left(\mathbf{x},\mathbf{x}^{(1)}\right),R\left(\mathbf{x},\mathbf{x}^{(2)}\right),\cdots,R\left(\mathbf{x},\mathbf{x}^{(n_s)}\right)\right]^T \tag{18}$$

Additionally, the Gaussian correlation function is employed in this work:

$$R\left(x^i,x^j\right) = \exp\left[-\sum_{k=1}^{n_{dv}}\theta_k\left|x_k^i - x_k^j\right|^2\right] \tag{19}$$

In Eq. 17, $\hat{\beta}$ is estimated using Eq. 20:

$$\hat{\beta} = \left(\mathbf{f}^T\mathbf{R}^{-1}\mathbf{f}\right)^{-1}\mathbf{f}^T\mathbf{R}^{-1}\mathbf{y} \tag{20}$$

The estimate of the variance $\hat{\sigma}^2$, between the underlying global model $\hat{\beta}$ and $\mathbf{y}$ is estimated using Eq. 21:

$$\hat{\sigma}^2 = \left[\left(\mathbf{y} - \mathbf{f}\hat{\beta}\right)^T\mathbf{R}^{-1}\left(\mathbf{y} - \mathbf{f}\hat{\beta}\right)\right]\Big/ n_s \tag{21}$$

where $f(\mathbf{x})$ is assumed to be the constant $\hat{\beta}$. The maximum likelihood estimates for the θ_k in Eq. 19, used to fit a Kriging model are obtained by solving Eq. 22:

$$\max_{\theta_k>0}\Phi(\theta_k) = -\left[n_s\ln\left(\hat{\sigma}^2\right) + \ln|\mathbf{R}|\right]\Big/ 2 \tag{22}$$

where both $\hat{\sigma}^2$ and $\mathbf{R}$ are functions of θ_k . While any value for the θ_k create an interpolative Kriging model, the "best" Kriging model is found by solving the *k*-dimensional unconstrained, nonlinear, optimization problem given by Eq. 22.

The accuracy of the prediction value largely depends on the distance from sample points.

Intuitively speaking, the closer point $\mathbf{x}$ to the sample point, the more accurate is the prediction $\hat{y}$. This intuition is expressed as

$$s^2(\mathbf{x}) = \hat{\sigma}^2\left[1 - \mathbf{r}^T\mathbf{R}^{-1}\mathbf{r} + \frac{\left(\mathbf{1} - \mathbf{1}\mathbf{R}^{-1}\mathbf{r}\right)^2}{\mathbf{1}^T\mathbf{R}^{-1}\mathbf{1}}\right] \tag{23}$$

where $s^2(\mathbf{x})$ is the mean squared error of the predictor and it indicates the uncertainty at the estimation point. The root mean squared error (RSME) is expressed as $s = \sqrt{s^2(\mathbf{x})}$.

Optimization Method

At the stage of computing optimization, we first select 40 sample points in the design space by Optimal Latin Hypercube Sampling method (OLHS) design, and use the Kriging model instead of huge numerical calculation to make quick evaluation. Finally, the genetic algorithm NSGA-II (Deb et al.,2002), is selected as the optimization method, and after 300×200 individual evolutions, the ideal optimization hull form is obtained.

HULL FORM OPTIMIZATION PROBLEM

Objective Function

The optimal calculation in this paper takes the KCS as the parent ship, which has the ship main dimensions of *L*=7.3577m, *B*=1.03m, *D*=0.346m, and the model can be seen in Fig. 4.

Fig. 4 Ship hull form of KCS

For instance, we can optimize a ship hull form considering its wave-making resistance, and *F* represents the average resistance of the hull at one or some different speeds. For traditional hull form optimization problem, the objective function is usually like Eq. 24 or Eq. 25.

$$\min \quad F = F\left(Fr = 0.26\right)\times 1 \tag{24}$$

$$\min \quad F = F_1\left(Fr = 0.2\right)\times\omega_1 + F_2\left(Fr = 0.3\right)\times\omega_2 \tag{25}$$

where $0 \le \omega_1 \le 1, 0 \le \omega_2 \le 1, \omega_1 + \omega_2 = 1$.

In fact, the ship is unlikely to sail at a certain speed in different needs or environmental conditions. If we consider the average resistance in a time period, we have

$$\overline{F} = \frac{F_1\Delta t_1 + F_2\Delta t_2 + \cdots + F_n\Delta t_n}{T} = \sum_{i=1}^{n}F_i\frac{\Delta t_i}{T} = \sum_{i=1}^{n}F_i p_i \tag{26}$$

Here, p_i represents the frequency of the speed's occurrence. We can assume that the sailing speed fluctuates up and down at the design speed(*Fr*=0.26), and its probability density function is normal distribution:

$$f(Fr) = Ae^{\frac{(Fr-0.26)^2}{2\times 0.075^2}} \tag{27}$$

In Eq. 27, *A* ensures that $\int_{0.18}^{0.34} f(Fr)\,\mathrm{d}\,Fr = 1$.

Therefore, the objective function here goes to

$$\min F\left(x_1,x_2,x_3,x_4\right) = \int_{0.18}^{0.34}F^*\left(x_1,x_2,x_3,x_4,Fr\right)f(Fr)\,\mathrm{d}\,Fr \tag{28}$$

It can be easily found that Eq. 24 and Eq.25 are both the special forms of Eq. 28, that is to say, the problem we come up with is a more general form.

Design Variables

Optimization variables are used to control the free variation of the ship form in the design space. Ship transformation method in this paper is FFD method, involving two lattices (shown in Fig. 5) at the bulbous bow and stern parts. Red points are movable while green points are fixed.

Four optimization design variables *X1, Y1, Z1, Y2* are summed up. The first 3 variables control the change of the bulbous bow surface in three directions: *x, y* and *z*. The last variable controls the change of the stern surface of the ship in the *y* direction. In order to ensure that the ship is within a reasonable range, the range of the variables is specified in Table 1.

For instance, if *X1*=+0.005, then all the red points in Fig. 5(a) move along the *x*-axis with a distance of +0.005m at the same time.

Table 1. The range of the 4 variables

	Variables	Min	Max
Lattice-1	*X1*	-0.01	0.01
	Y1	-0.007	0.007
	Z1	-0.015	0.015
Lattice-2	*Y2*	-0.01	0.01

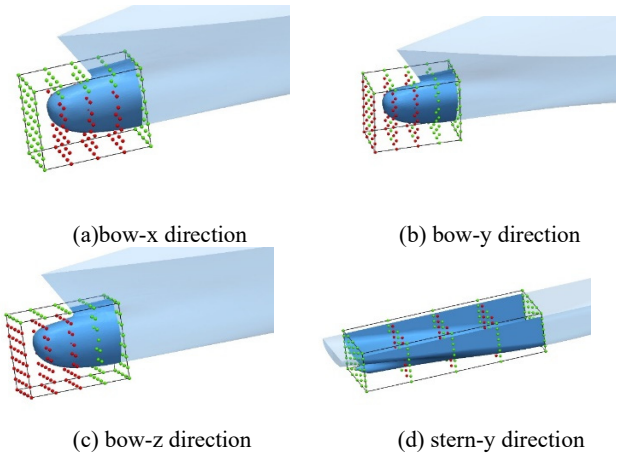

(a)bow-x direction (b) bow-y direction

(c) bow-z direction (d) stern-y direction

Fig. 5 Schematic diagram of FFD method application (Lattice and layout of control points)

Optimization results and analysis

We firstly use the OLHS method to generate 40 sample points for 40 new hull forms which are uniformly distributed in the design space, and calculate the wave-making resistance in a series of speeds (Fr=0.18,0.2,0.22,0.24,0.26,0.28,0.3,0.32,0.34) separately; then we set Kriging approximation model of $F^*(x_1,x_2,x_3,x_4,Fr)$ to do the optimization calculation. Through leave-one-out cross validation, we can see the accuracy of the constructed Kriging surrogate model $F^*(x_1,x_2,x_3,x_4,Fr)$,which is shown in Fig. 6.

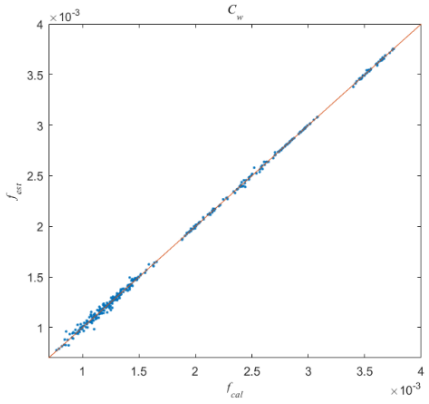

Fig. 6 Cross validation of Kriging approximation model

According to Eq. 28, we can obtain the integral that is the function of hull form transformation values. Finally, we use genetic algorithm NSGA- II as the optimization method, and calculate the 300×200 individuals to get the optimization results, that is, the average wave-making resistance.

Table 2. The comparisons of the shape parameters of initial and optimal hulls

	Variables	Initial	Optimal
Lattice-1	*X1*	0	-0.009
	Y1	0	0.004
	Z1	0	0.009
Lattice-2	*Y2*	0	-0.006

The hull lines comparisons are shown in Fig. 7.

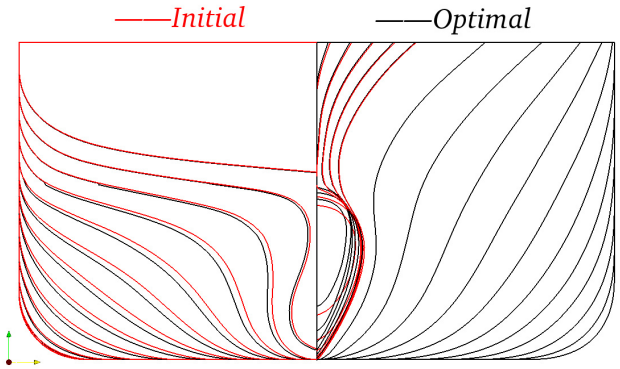

Fig. 7 Hull line comparisons

We can see from Fig. 7 that the bulbous of the optimal hull is thinner and higher than the initial one, and stern parts of the optimal hull is a little fatter than the initial one.

Finally, we calculate the wave-making coefficients in different Froude numbers, then we can obtain Fig. 8, which shows that the optimal hull has lower wave-making coefficients at full speed range from *Fr*=0.18 to *Fr*=0.34, especially in smaller Froude numbers.

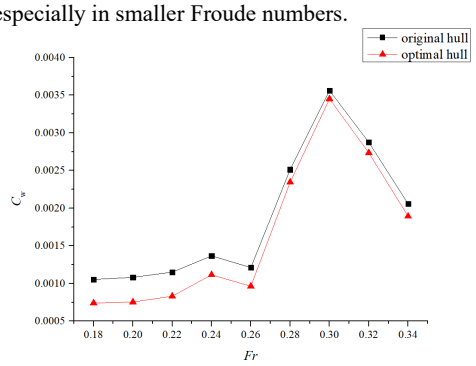

Fig. 8 Wave-making coefficients at full speed range

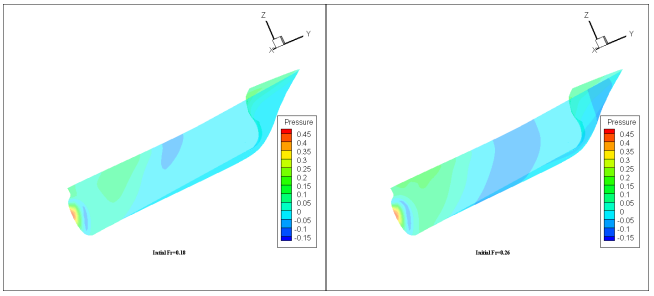

(a) *Fr*=0.18 (b) *Fr*=0.26

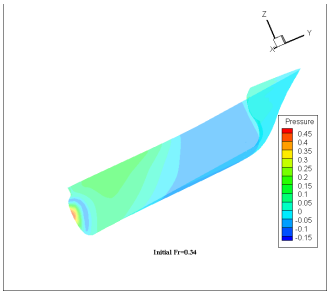

(c) *Fr*=0.34

Fig. 9 Pressure distributions of initial hull in different Froude numbers

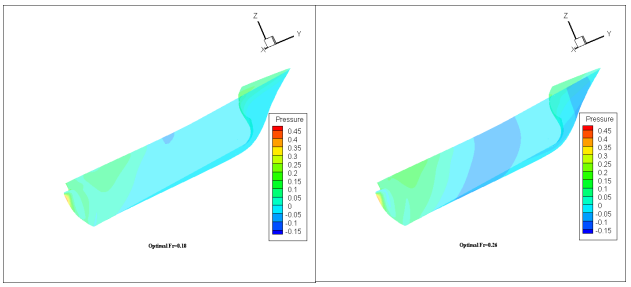

(a) *Fr*=0.18 (b) *Fr*=0.26

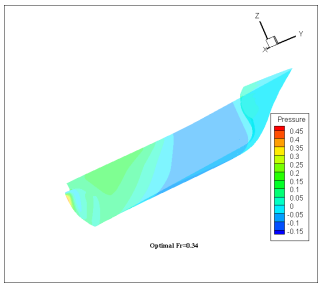

(c) *Fr*=0.34

Fig. 10 Pressure distributions of optimal hull in different Froude numbers

Seen from Fig. 9~10, the bulbous of the optimal hull has smaller high pressure and low pressure regions, which mean the lower wave-making resistances.

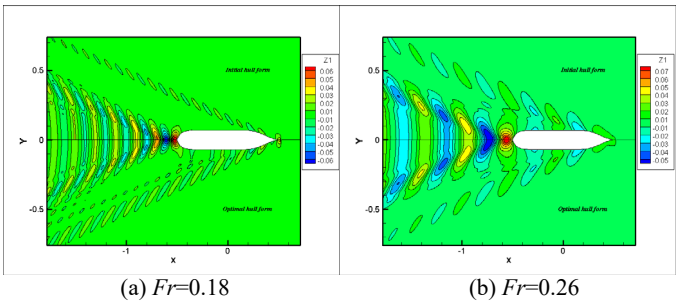

(a) *Fr*=0.18 (b) *Fr*=0.26

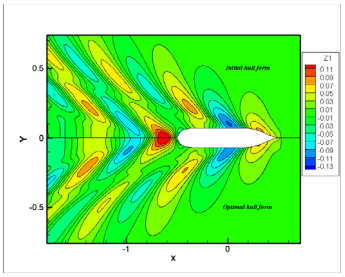

(c) *Fr*=0.34

Fig. 11 Free surface wave elevation comparisons in different Froude numbers

From Fig. 11, the free surface elevations of the optimal hull are smaller, especially in Fr=0.34, which also reflect the lower wave-making resistances.

CONCLUSIONS

In this paper, the KRISO Container Ship is considered as the parent ship. The hull form can be globally deformed while the wetted surface area and displacement are constrained within a certain range. The probability distribution function of the speed is given and the mathematical expectation of total resistance in calm water at full speed range is regarded as the objective function. Kriging approximate model is constructed which can reduce the computational cost. Finally, the single-objective genetic algorithm is taken as the optimization technique leading to an optimal ship considering full speed range. The results show that the resistance performance of the optimal ship at full speed range is much better.

The whole optimization process is implemented based on in-house optimization solver OPTShip-SJTU and potential theory-based solver NMShip-SJTU. It turns out that it's essential to consider the wave-making resistance at full speed range because of the real environment conditions and OPTShip-SJTU has practical applications in the aspect of probability optimization of ship hydrodynamic performances.

In the future, we will focus more on the performances of seakeeping and maneuvering using high-fidelity CFD tools.

ACKNOWLEDGEMENTS

This work is supported by the National Natural Science Foundation of China (51490675, 11432009, 51579145), Chang Jiang Scholars Program (T2014099), Shanghai Excellent Academic Leaders Program (17XD1402300), Program for Professor of Special Appointment (Eastern Scholar) at Shanghai Institutions of Higher Learning (2013022), Innovative Special Project of Numerical Tank of Ministry of Industry and Information Technology of China (2016-23/09) and Lloyd's Register Foundation for doctoral student, to which the authors are most grateful.

REFERENCES

Deb, K, Agrawal, S, Pratap, A, Meyarivan, T (2002). "A Fast and Elitist Multi-Objective Genetic Algorithm: NSGA-II," *IEEE Transactions on Evolutionary Computation*, 6(2):182-197.

Kim, H, Yang, C, Chun, HH (2009). "Hydrodynamic Optimization of a Modern Container Ship Using Variable Fidelity Models," *Proc 19th Int Offshore and Polar Eng Conf*, Osaka, Japan, ISOPE.

Liu, XW, Wan, DC (2017). "Numerical Analysis of Wave Interference Among the Demihulls of the High-Speed Quadramarans," *Shipbuilding China*, 58(1):140-151.

Noblesse, F, Huang, FX, Yang, C (2013). "The Neumann-Michell Theory of Ship Waves," *J Eng Math*,79(1): 51-71.

Sederberg, TW, Parry, SR (1986). "Free-form Deformation of Solid Geometric Primitives," *Computers & Graphics*, 20(4):151-160.

Sykulski, AM, Adams, NM, Jennings, NR (2011). "On-Line Adaptation of Exploration in the One-Armed Bandit with Covariates Problem," *9th Int Conf on Machine Learning and Application*, IEEE, 459-464.

Wu, JW, Liu, XY, Zhao, M, Wan, DC (2017). "Neumann-Michell Theory-based Multi-objective Optimization of Hull Form for a Naval Surface Combatant," *Applied Ocean Res*, 63:129-141.

Yang, C, Huang, FX, Noblesse, F (2013). "Practical Evaluation of the Drag of a Ship for Design and Optimization," *J Hydrodyn*, 25(5):645-654.

Zhang, CL, He, JY, Ma, C, Wan, DC (2015). "Validation of the Neumann-Michell Theory for Two Catamarans," *Proc 25th Int Offshore and Polar Eng Conf*, Kona, Big Island, Hawaii, USA, ISOPE, June 21-26, 2015, 1018-1024.

Zhang, CL, Wan, DC (2015). *The Manual of NMShip-SJTU Solver*, Technique Report No. 2015SR011407, Shanghai Jiao Tong University, Shanghai, China.